

1 Estimation of vertical land movement rates along the 2 coasts of the Gulf of Mexico over the past decades

3 C. LETETREL¹, M. KARPYTCHEV¹, M-N. BOUIN², M. MARCOS³, A. SANTAMARÍA-GÓMEZ¹⁻⁴,
4 AND G. WÖPPELMANN¹

5 ¹UMR 7266 LIENSS, Université de La Rochelle – CNRS, 2 rue Olympe de Gouge, 17000 La
6 Rochelle, France

7 ²CNRM/CMM, Météo-France, 13 rue du Chatellier, 29228 Brest, France

8 ³IMEDEA (CSIC-UIB), Miquel Marquès, 07190 Esporles, Spain

9 ⁴Instituto Geográfico Nacional, Cerro de la Palera, s/n, 19141, Yebes, Spain

10

11 **Corresponding author:** Camille Letetrel

12 Tel: +33 5 46 50 76 31

13 Fax: +33 5 46 45 82 49

14 Address: Bat. ILE, 2 rue Olympe de Gouges, 17042 La Rochelle Cedex, France

15 Email: camille.letetrel@univ-lr.fr.

16

17 Suggested reviewers:

18 W. Bosch (bosch@dgfi.badw.de)

19 A. Cazenave (anny.cazenave@legos.obs-mip.fr)

20 S. Holgate (simonh@pol.ac.uk)

21 C.Y. Kuo (kuo70@mail.ncku.edu.tw),

22 C.K. Shum (ckshum@osu.edu)

23 P. L. Woodworth (plw@pol.ac.uk)

24 P. Moore (philip.moore@ncl.ac.uk)

25 **Abstract.**

26 We estimated the vertical land movement rates at tide gauge stations along the Gulf of Mexico (GOM) coasts. A
27 novel approach suggested by Kuo et al. (2004, 2008) for combining satellite altimetry and tide gauge data was
28 applied. The obtained vertical land motion rates were compared with the GPS vertical velocities measured at
29 Galveston, Grand Isle, Dauphin Island, Pensacola and Key West stations. The estimated vertical rates range from
30 slow subsidence in the South of Florida and Veracruz to high subsidence rates in Texas and Louisiana where
31 some of the tide gauges subside at the rate of up to 7 mm/yr. A small but noticeable uplift in the NE of the Gulf
32 was detected at Cedar Key and Apalachicola and a very low subsidence at Pensacola tide gauge. We suppose
33 there are some local tectonic processes which contribute significantly to the land movement at these stations.
34 Comparison with the post-glacial rebound model ICE5G-VM2 predictions shows that the drivers of the
35 subsidence on the GOM shelf are of local nature. The resulted absolute sea level rise along the GOM coast was
36 estimated to be about 2.0 ± 0.4 mm/yr.

37

38 **Key words:** *Vertical land motion, Satellite altimetry, Tide gauge, GPS, Gulf of Mexico.*

39

40 **1. Introduction**

41 The low-lying coasts of the Gulf of Mexico (GOM) are a site of a large variety of ecosystems
42 and human communities that are highly vulnerable to sea level changes. Sea level rise in these
43 areas is a major problem for coastal strategy planning as the population of the five states of
44 the U.S for example. Gulf coast has been projected by the Census Bureau to increase nearly
45 40% from 1995 to 2025 (Crosset et al. 2004). An accurate estimate of the long term trends in
46 relative sea-level rise (SLR) along the Gulf coasts is thus of primary importance for
47 appraising the risks associated with the vulnerability of low-lying areas.

48 The relative sea level fluctuations include both absolute sea level changes and vertical land
49 motion that can be due to glacial isostatic adjustment (GIA), tectonic processes or coastal
50 subsidence or uplift provoked by anthropogenic factors. The rates of the relative SLR in the
51 GOM range from about 1 mm/yr at Veracruz, Mexico, to nearly 10 mm/yr at Grand Isle, in
52 the Mississippi delta (Douglas, 2005). This large variability is mostly due to the subsidence of
53 the northern GOM induced by extraction of hydrocarbons, groundwater withdrawal, land
54 reclamation and sedimentation (Emery and Aubrey, 1991; Douglas, 2005). As to the vertical
55 land movements due to GIA, they are spatially uniform along the GOM coasts and have
56 amplitude less than 1 mm/yr of subsidence (Peltier, 2004). No significant tectonic activity
57 was reported along the northern Gulf coast, the Gulf seismicity being relatively low
58 (Nicholson and Wesson, 1990; Gonzalez and Törnqvist, 2006; Törnqvist, et al. 2006) although
59 the coast is not seismically quiescent (Lopez, 1991).

60 In general, the coast of the Gulf of Mexico is exposed to problematic situations that can be
61 categorized into two different processes: 1) coastal erosion; and 2) loss of wetlands (Boesch,
62 et al. 1994; Davis, 2011). Both of these processes are at least partly due to absolute sea level

63 rise exacerbated by vertical land movements (Davis, 2011). This issue particularly concerns
64 the most vulnerable parts of Louisiana and eastern Texas coasts.

65 Several techniques can be used to monitor the vertical land motion. Tide gauges measure sea
66 level relative to a local reference point attached to the land upon which the gauges are
67 grounded at the coast. Differences between tide gauge sea level records have been used in the
68 past to provide a map of relative land movement consistent with previous geological
69 knowledge of the area (Emery and Aubrey, 1991). However, in the context of sea level rise,
70 this approach does not attain accuracy in estimating vertical land movement rates that is
71 required by the coastal community planning. In contrast to the tide gauge data which are
72 measurements of sea level relative to land datum, space geodetic techniques have been used to
73 estimate the geocentric vertical motion relative to the Terrestrial Frame. In the recent years,
74 Global Positioning System (GPS) has become a commonly used geodetic technique due to its
75 high precision, ease of use and affordable equipment. The use of GPS vertical velocities in
76 combination with tide gauge records has provided worthwhile results on the global scale
77 (Wöppelmann et al. 2007). However, the GPS network is heterogeneous and the recording
78 period is sometimes too short to estimate a stable trend in land movement. Many problems
79 remain to be solved. For instance, the importance of a stable and accurate reference frame
80 over decades has repeatedly been underscored (e.g., Beckley et al. 2007; Blewitt et al. 2010),
81 and has become the dominant limiting factor for reducing uncertainties in the recent global
82 sea-level trend estimates (Collilieux and Wöppelmann 2011). Since the early 1990's, satellite
83 altimetry provides an accurate absolute measurement of sea surface height. Mitchum (1994)
84 proposed to calibrate the time-dependent drift in satellite data by comparing the altimetry and
85 tide gauge measurements. As the length and quality of satellite measurements improve
86 constantly, Mitchum (1998) turned the calibration problem into a method for estimating
87 vertical land motion by differencing absolute sea level heights derived from the satellite

88 altimetry and the tide gauge records. To the extent the sea level signals are coherent; the
89 difference “altimetry minus tide gauge” is a measure of vertical land motion at the gauge. The
90 approach has also been explored by Cazenave et al. (1999), Nerem and Mitchum (2002),
91 Garcia et al. (2007) among others.

92 Buble et al. (2010) developed the method proposed earlier by Davis et al. (1999) to separate
93 common-mode relative sea level from spatially variable signals. They used the observations
94 from tide gauges colocated with continuous GPS (CGPS) stations to investigate crustal
95 deformation and absolute sea level changes along the eastern margin of the Adriatic Sea.

96 To overcome the space coverage limitation of GPS stations and restrictions due to the short
97 length of the altimetry time series, Kuo et al. (2004, 2008) have significantly improved the
98 basic method used by Cazenave et al. (1999) and Nerem and Mitchum (2002), hereafter
99 referred to as the direct approach. As in the direct method, the general idea of the Kuo’s
100 approach consists in subtracting the tide gauge data relative to the coast from the geocentric
101 satellite altimetry data. The novelty of this method is in setting some complementary
102 constraints on the estimated “altimetry – minus tide gauge” differences. Kuo et al. (2004)
103 assumed that the trend of absolute or geocentric sea level variations is the same at the
104 neighboring tide gauges (Kuo et al. 2004). The method was successfully applied for
105 determining land motion and absolute sea level trend in lakes (Kuo, 2005), the closed seas as
106 the Baltic Sea (Kuo, et al., 2004) and the Mediterranean Sea (Woppelmann and Marcos, 2012)
107 and along the Alaska shelf (Kuo, 2005). In this paper, we applied the Kuo et al. (2004)
108 approach in the estimation of vertical land movement along the coasts of the GOM. At the low
109 enough frequency, the flow on the GOM shelf is quasi-geostrophic (Li and Clarke, 2005) and
110 the absolute sea level signal should be nearly constant along the shelf. Although the wind
111 forcing introduces spatial variability in the absolute sea level signal at the interannual
112 frequencies (Li and Clarke, 2005), its effect seems to be negligible over the periods longer

113 than 5 yr (Douglas, 2005). Thus, the interdecadal absolute sea level fluctuations and
114 especially the trend over the last 50 years are expected to be coherent and in phase over the
115 entire GOM shelf.

116 The Kuo et al. approach was proved to be superior in terms of precision and accuracy than the
117 direct approach that is still in use (e.g., Garcia et al. 2007; Ray et al. 2010; Braitenberg et al.
118 2011; Trisirisatayawong et al. 2011). Applying this technique to the Gulf of Mexico shelf is
119 interesting for several reasons: first, the Gulf coast is affected by land motion of large
120 variability (Davis, 2011). Secondly, the tide gauge records along the North coast are of high
121 quality that allows getting accurate estimates of relative sea level trends . Third, the
122 robustness of the method can be checked against the independent GPS vertical velocities in
123 the GOM from the latest ULR solution (Santamaría-Gómez et al. 2012). And finally, the
124 results will provide estimates of absolute vertical motion responsible for relative sea level rise
125 in a vulnerable area affected by: (1) the compaction of sediments carried out by the
126 Mississippi river, (2) local tectonic processes as salt migration or crustal faulting or (3) human
127 activity mostly associated with withdrawals of fluids and the petroleum engineering.

128 Our investigation begins in Section 2 by reviewing available tide gauge records, the satellite
129 altimetry data and continuous GPS stations co-located at tide gauge stations in the Gulf of
130 Mexico. Section 3 describes the direct method employed by Mitchum (1998), Cazenave et al.
131 (1999) and presents the approach of Kuo et al. (2004, 2008). Section 4 discusses the estimated
132 vertical land motion rates and compares them to the prediction of the last version v1.3of ICE-
133 5G-VM2 model (Peltier, 2004) and to the GPS vertical rates. Section 5 concludes the study.

134

135

136

137 **2. Data sets**

138 **2.1. Tide gauges**

139 The tide gauge records used in this study are monthly averaged time series from the ‘Revised
140 Local Reference (RLR)’ dataset of the Permanent Service for Mean Sea Level (PSMSL,
141 available at <http://www.pol.ac.uk/psmsl>). The RLR is the most appropriate dataset for the long
142 term trend studies as its records were previously checked and corrected for local datum
143 stability relative to benchmarks in their nearest vicinity (Holgate, et al. 2013). We focused on
144 RLR records from the Gulf of Mexico with a sufficient number of observations to determine
145 long-term relative sea level rates that are believed to represent the long-term climate
146 contributions plus the movement of the land on which the tide gauges are grounded. For 40-
147 year long tide gauge records, the standard errors of the linear trends are typically of 0.5 mm/yr
148 (Douglas 1991, 2001). Tide gauge records were rejected if they did not contain more than
149 85% of valid data within a time span of at least 40 years. The tide gauge records were
150 truncated at December 2011 (section 2.3). The names of tidal stations used, along with their
151 location, period of operation and percentage of data gaps are listed clockwise around the Gulf
152 of Mexico from Veracruz, Mexico, to Key West, Florida in Table 1. Fig 1 shows the location
153 of the 15 selected tide gauge records. Most are located along the northern coast of the Gulf of
154 Mexico. The Galveston II record is the longest: it extends back to 1908. Note that Galveston
155 II is located 2.8 km apart from Galveston I. Both Galveston stations have been operating
156 simultaneously since 1957.

157

Table 1

158 Table 1: Tide gauge data used in this study from the PSMSL. Trend values and standard errors of the trends (in
159 mm/yr) are derived from a robust linear regression (Street et al. 1988) over the entire data span available at each
160 tide gauge. Approximate distances to the nearby continuous GPS station are in km.

161

162 **2.2. Satellite altimetry**

163 The satellite altimetry data used in this study were weekly gridded sea level anomaly (SLA)
164 fields computed from a merged multi-mission solution of AVISO
165 (<http://www.aviso.oceanobs.com/duacs/>). The SLA were produced by combining data from
166 several satellite altimetry missions, namely: Topex/Poseidon (T/P) over the period 1992-2002;
167 Jason-1 from April 2002 to October 2011; Jason-2 from October 2008 to December 2011;
168 ERS-1/2 from October 1992 to April 2003 with a lack of ERS-1 data from January 1994 to
169 March 1995; and ENVISAT from October 2002 to December 2011. The resolution of the SLA
170 altimetry fields is $1/3^\circ \times 1/3^\circ$ resulting in a total of 2036 points covering the region of the Gulf
171 of Mexico within the limits of 18.26 N to 32.09 N degrees in latitude and 80.67 W to 98.33 W
172 degrees in longitude (Figure 1).

173 To minimize aliasing effects, an atmospheric correction was applied along with the
174 corrections for geophysical (e.g., tides and sea state) and instrumental effects (Volkov et al.
175 2007). In the AVISO dataset update (September 2010), the standard Inverted Barometer (IB)
176 correction was complemented with corrections from MOG2D barotropic model (Carrère and
177 Lyard 2003), which improves the representation of high frequency atmospheric forcing
178 effects. The AVISO update of September 2010 also incorporated the reprocessed T/P and
179 Jason-1 orbits for the entire time series, which used the ITRF2008 terrestrial reference frame
180 (Altamimi et al. 2011), and has proven to be substantially superior to the previous 1995-era
181 frame products (e.g., Beckley et al. 2007).

182 To be consistent with the tide gauge data, we, first, chose to add back the atmospheric
183 component of sea level to the gridded SLA by using the MOG2D corrections kindly provided
184 by CLS Space Oceanography Division (Carrère and Lyard 2003). Then we constructed the
185 monthly SLA from this set of data. The influence of the atmospheric forcing on sea level at
186 the interannual and lower frequencies is supposed to be similar at tide gauge sites and the

187 corresponding altimetry points. Also, as pointed by Kuo et al (2008), the effect of common
188 noise in tide gauge records and in altimetry data will be attenuated as it is the difference
189 (trend of altimetry – trend of tidal record) that stands in equation 3 (see Section 3.2).

190 To be consistent with tide gauge records, no GIA correction was applied to the altimetry
191 dataset. The mean seasonal signals (annual and semiannual) from both the SLA and tide
192 gauge data were also removed by subtracting the average of each calendar month.

193 **Figure 1**

194 Fig.1: Location of tide gauge records in the northern Gulf of Mexico (circles) with more than 40 years of data at
195 PSMSL and grid points from AVISO altimetry data used in this study. The background colours represent absolute
196 sea level rates over the common period October 1992 to December 2011. The underlined tide gauge names
197 denote the co-location with a nearby continuous GPS station.

198 The 19-year absolute sea level trends in the deep waters of the Gulf (Fig.1) are not spatially
199 uniform and reflect the dominant influence of the Loop Current variability on the trend
200 estimates (Sturges and Evans 1983; Li and Clarke 2005; Oey et al. 2005). The pronounced
201 variations in the absolute sea level and a short time interval make it difficult to estimate the
202 trends accurately. In other words, the records are not yet long enough and are too noisy to
203 provide an accurate and robust estimate of the absolute sea level trend in this region. Hughes
204 and Williams (2010) demonstrated (in fig. 7.b) that more than 18 years of observations are
205 needed to estimate the linear trend the GOM coast with the uncertainty < 1 mm/yr . The
206 objective of achieving more accurate trend estimates is also the reasons for combining tide
207 gauge records with the altimetry data. The main differences between tide gauge and
208 altimetry-derived sea level rates (Fig.1) mostly result from the vertical movement of the coast.
209 This is particular true in the north-western part of the Gulf of Mexico, in Texas and in
210 Louisiana where the important contribution of sediment loading and water pumping was
211 identified in previous studies (Kolker et al. 2011).

212 **2.3. Continuous GPS stations at tide gauges**

213 Recent studies have shown that accurate vertical velocities can be estimated from continuous
214 GPS stations with sufficient accuracy for monitoring land movements at tide gauges in a
215 global geocentric reference frame common to satellite altimetry data (e.g., Wöppelmann et al.
216 2007; 2009; Bouin and Wöppelmann, 2010). However, any change in the equipment, in the
217 geocentric datum, in the parameterization or in the models used to analyze the GPS data
218 might affect the GPS-derived estimates of the vertical land movement. The use of a
219 consistent analysis strategy throughout the whole GPS observation data span was
220 demonstrated to be mandatory to prevent station position time series from being contaminated
221 with errors that could make questionable any interpretation of the GPS-derived velocities in
222 terms of ground displacement.

223 In this study, we used GPS velocities from the latest solution produced by the Université de
224 La Rochelle (ULR). The solution was completed using a consistent GPS reprocessing strategy
225 spanning 13 years of data from January 1995 to December 2010. Both GPS reprocessing and
226 vertical velocity estimation strategies are described in Santamaría-Gómez et al. (2012).

227 Five continuous GPS stations of the latest ULR solution are located near a tide gauge in the
228 Gulf of Mexico (Table 1): Galveston (GAL1); Grand Isle (GRIS); Dauphin Island (MOB1);
229 Pensacola (PCLA); and Key West (KYW1). All these stations have been in continuous
230 operation (without noticeable position discontinuities) for at least more than 3.5 years,
231 necessary to reduce the impact of seasonal oscillations on rate estimates. Station vertical
232 velocities were estimated in the ITRF2008 reference frame (Altamimi et al. 2011). Realistic
233 formal uncertainties were obtained by analysing the noise content of the weekly GPS position
234 time series (Santamaría-Gómez et al. 2011). The results of the Gulf of Mexico stations are
235 reported in the fourth column of Table 2.

236 The Dauphin Island GPS station (MOB1) was discarded from the analysis below (Table 2). A
 237 detailed examination of the local environment shows that the GPS antenna is 5.5 km away
 238 from the tide gauge on the opposite side of the estuary
 239 (<http://www.sonel.org/spip.php?page=gps&idStation=2972.php>). Consequently, serious
 240 concerns on the representativeness and the reliability of the estimated vertical velocity of the
 241 GPS station MOB1 nearby Dauphin Island were raised and prevented us from using it in the
 242 study.

243

244 **3. Estimation of vertical land movement rates**

245 **3.1. Combining satellite altimetry and tide gauge data: a direct** 246 **approach**

247 A direct approach developed by Cazenave et al. (1999) and Mitchum (1998) to determine land
 248 movements at the coast consists in subtracting altimetry-derived sea surface heights from tide
 249 gauge records over their common period. The rates of relative and absolute (geocentric) sea
 250 level changes as observed by tide gauges, \dot{S} , and by satellite altimeters, \dot{g} , can be written as
 251 follows:

$$\begin{aligned}
 \dot{S}(\lambda, \varphi) &= \dot{T}(\lambda, \varphi) - \dot{u}(\lambda, \varphi) + t_{error}(\lambda, \varphi) \\
 \dot{g}(\lambda, \varphi) &= \dot{T}(\lambda, \varphi) + a_{error}(\lambda, \varphi)
 \end{aligned}
 \tag{E1}$$

253 where $\dot{u}(\lambda, \varphi)$ is the rate of geocentric vertical land movement (at longitude, λ , and latitude,
 254 φ), $T(\lambda, \varphi)$ represents all physical contributions to the absolute rate of sea level change, and
 255 t_{error} and a_{error} are the drifts associated with both the tide gauge and the satellite altimeter
 256 instruments, respectively. Provided that both instruments capture the same absolute sea level

257 signal, T , and that the drifts t_{error} and a_{error} are small and negligible, the absolute sea level
258 signal T cancel in the difference $(\dot{g} - \dot{S})$; leaving only vertical land movement, \dot{u} , as it is
259 recorded by the tide gauge but not by the satellite altimeter, $u > 0$ corresponds to uplift and $u < 0$
260 to subsidence.

$$261 \quad \dot{u}(\lambda, \varphi) = \dot{g}(\lambda, \varphi) - \dot{S}(\lambda, \varphi) \quad (\text{E2})$$

262 This assumption is valid only if a good match between satellite altimetry and tide gauge sea
263 level time series can be achieved. Thus, the importance of ensuring the consistency of both
264 sources of sea level data, especially the temporal sampling, the overlapping of the time series
265 and the application of common corrections, whatever the performance of the corrections could
266 be as correction errors will cancel in the differentiation if they are identical (section 2). In
267 addition, it is worth reminding that continuous efforts are undertaken to monitor and correct
268 the altimetry data for instrumental biases, in particular due to changes in altimeters from
269 consecutive satellite missions (e.g., Ablain et al. 2009). A similar remark applies to the tide
270 gauge data from the PSMSL (Woodworth and Player, 2003). Consequently, we neglected the
271 terms t_{error} and a_{error} in equation (E1).

272 In this study, the minimum overlap between the satellite altimetry and tide gauge monthly
273 time series was of 12 years. Estimated VLM trends from the direct approach are provided in
274 Table 2 (column 2).

275 **3.2. Advanced method: Kuo et al. approach**

276 Whatever the differences in the implementation of the idea, the above mentioned studies only
277 used tide gauge data during the satellite altimetry time span. The tide gauge records prior to
278 the satellite altimetry era were not considered, even if available. To incorporate the invaluable
279 information embedded in the historical records, Kuo et al. (2004) devised a novel approach by

280 adding constraint equations derived from long term tide gauge records (> 40 years) to the
 281 classical algorithm. These constraints are expressed through the differential rates of vertical
 282 land movement, $\dot{r}u_{ij}$, between pairs of tide gauges, i and j, which can be expanded using (E1)
 283 as follows:

$$\begin{aligned}
 \dot{r}u_{ij} &= \dot{u}_i(\lambda_i, \varphi_i) - \dot{u}_j(\lambda_j, \varphi_j) \\
 &= T_i(\lambda_i, \varphi_i) - \dot{S}_i(\lambda_i, \varphi_i) - T_j(\lambda_j, \varphi_j) + \dot{S}_j(\lambda_j, \varphi_j) + t_{ij,error}
 \end{aligned}
 \tag{E3}$$

285 Provided that two neighbouring tide gauges capture the same absolute sea level signals, T_i and
 286 T_j , and that the total instrumental drifts, summed up in $t_{ij,error}$, are negligible, the differential
 287 rate of two adjacent tide gauge time series largely reflects the difference in vertical land
 288 movement at the sites.

$$\dot{r}u_{ij} = \dot{u}_i(\lambda_i, \varphi_i) - \dot{u}_j(\lambda_j, \varphi_j) \approx \dot{S}_j(\lambda_j, \varphi_j) - \dot{S}_i(\lambda_i, \varphi_i)
 \tag{E4}$$

290 To be more rigorous, the equation (E4) is valid only for the period covered by tide gauge, and
 291 should be rewritten as follow:

$$\dot{r}u_{ij} = \dot{u}_i(\lambda_i, \varphi_i) - \dot{u}_j(\lambda_j, \varphi_j) \approx \dot{S}_j^{TG}(\lambda_j, \varphi_j) - \dot{S}_i^{TG}(\lambda_i, \varphi_i)
 \tag{E5},$$

293 where \dot{S}_i^{TG} and \dot{S}_j^{TG} are the rates of tide gauge records computed over their whole period.

294 Whereas the direct approach uses at most two decades of data to determine the land
 295 movements (satellite altimetry time span), equation (E5) imposes constraints on the rates of
 296 differential land movements based on the full length of the tide gauge records. This is slightly
 297 different compared to Kuo et al. who used the same time span of tide gauge records in order
 298 to reduce common-mode error. However, the land movement of the GOM coasts is
 299 dominated by local processes and hence is not really coherent. For example, Galveston is
 300 mostly driven by underground pumping, Grand Isle – by the Mississippi sediment loading etc.

301 The large scale coherent part of land movement due to post-glacial rebound is rather small
302 contrary to Scandinavia analysed by Kuo et al (2004). In other words, there is large
303 contribution of decadal variability due to land movement that is not common among the
304 GOM tide gauges As the low-frequency variability due to land movement dominates this
305 caused by absolute sea level variations, using the tide gauge records over their whole period is
306 more favourable for search of accurate relative sea level trend estimates in eq. (E5).
307 The equations (E2) and (E5) can be expressed in a matrix form that can be solved by the
308 constrained least squares minimization (Menke, 1989):

$$309 \quad \mathbf{Fm}=\mathbf{h}, \text{ with } \mathbf{F} = \begin{pmatrix} 1 & -1 & 0 & \dots & \dots & 0 \\ 0 & 1 & -1 & \ddots & & \vdots \\ \vdots & \ddots & \ddots & \ddots & \ddots & \vdots \\ \vdots & & \ddots & \ddots & \ddots & 0 \\ 0 & \dots & \dots & 0 & 1 & -1 \end{pmatrix}, \mathbf{m} = \begin{pmatrix} \bullet \\ u_1 \\ \bullet \\ u_2 \\ \vdots \\ \bullet \\ u_{n-1} \\ \bullet \\ u_n \end{pmatrix} \text{ and } \mathbf{h} = -\mathbf{F} \begin{pmatrix} \bullet \\ S_1^{TG} \\ \bullet \\ S_2^{TG} \\ \vdots \\ \bullet \\ S_{n-1}^{TG} \\ \bullet \\ S_n^{TG} \end{pmatrix} \quad (\text{E6});$$

310 with F being a n-1 x n matrix, n the number of tide gauge records selected.

311 And equation (E2) can be written in the form:

$$312 \quad \mathbf{Gm}=\mathbf{d}, \text{ avec } \mathbf{G} = \begin{pmatrix} \mathbf{1} & \mathbf{0} & \dots & \dots & \mathbf{0} \\ \mathbf{0} & \mathbf{1} & \mathbf{0} & \dots & \mathbf{0} \\ \vdots & & \ddots & & \vdots \\ \vdots & & & \ddots & \mathbf{0} \\ \mathbf{0} & \dots & \dots & \mathbf{0} & \mathbf{1} \end{pmatrix}, \mathbf{m} = \begin{pmatrix} \bullet \\ u_1 \\ \bullet \\ u_2 \\ \vdots \\ \bullet \\ u_n \end{pmatrix} \text{ et } \mathbf{d} = \begin{pmatrix} \bullet & \bullet^{SAT} \\ g_1 - S_1 & \bullet^{SAT} \\ \bullet & \bullet^{SAT} \\ g_2 - S_2 & \bullet^{SAT} \\ \vdots & \vdots \\ \bullet & \bullet^{SAT} \\ g_n - S_n & \bullet^{SAT} \end{pmatrix} \quad (\text{E7}),$$

313

314 with G being a n x n matrix, if we consider all pairs of stations selected. The direct approach
315 is restricted to equation (E7), considers only the satellite period. The approach proposed by
316 Kuo et al. (2004; 2008) constrains the equation (E7) by the equation (E6) including the tide
317 gauge period. To solve (E6)-(E7), we implemented the constraints by using Lagrange

318 multipliers (Letetrel, 2010 ; Woppelmann and Marcos 2012). Equations (E6) and (E7) were
 319 expressed as (Menke, 1989):

$$320 \begin{bmatrix} \mathbf{G}^T \mathbf{d} \\ \mathbf{h} \end{bmatrix} = \begin{bmatrix} \mathbf{G}^T \mathbf{G} & \mathbf{F}^T \\ \mathbf{F} & \mathbf{0} \end{bmatrix} \begin{bmatrix} \mathbf{m} \\ \mathbf{v} \end{bmatrix} + \mathbf{E} \quad (\text{E8}),$$

321 where \mathbf{v} is an $n-1$ column vector representing the Lagrange multipliers and \mathbf{E} is zero-mean
 322 column vector of random errors. Equation (E8) was solved by the generalized least mean
 323 square procedure (Menke, 1989). Equation (E8) is a linear system of the form $\mathbf{A} \cdot \mathbf{X} = \mathbf{Y}$ whose
 324 simple least squares solution is given by

325 $\mathbf{X} = (\mathbf{A}'\mathbf{A})^{-1} (\mathbf{A}'\mathbf{Y})$. If we follow the general least squares theory, the uncertainties of the term “
 326 \mathbf{m} ” can be estimated from the diagonal terms of the associated covariance matrix $(\mathbf{A}'\mathbf{W}\mathbf{A})^{-1}$

327 Where \mathbf{W} has the following form:

$$328 \left[(\mathbf{A}'\mathbf{A})^{-1} \mathbf{A}' \right]^2 \begin{bmatrix} E_g^2 + E_{sp}^2 \\ F^2 * E_s^2 \end{bmatrix}, \text{ where } E_g \text{ is the standard error of the linear trend of}$$

329 satellite time series, E_{sp} is the standard error of the linear trend of tide gauge time series over
 330 the altimeter period and E_s is the standard error of the linear trend of tide gauge time series
 331 over the tide gauge period.

332 The constraints from (E5) proved to be successful in the Baltic Sea, the Great Lakes and
 333 Alaska (Kuo et al. 2004, 2008), showing significantly reduced uncertainties in estimates of
 334 the vertical land movement rates compared with other studies using the direct approach.

335 These were assessed by comparing to external data from GPS solutions, suggesting that the
 336 assumption that the rates of absolute sea level variations are the same at nearby tide gauges
 337 holds particularly true in semi-enclosed seas or lakes. Kuo et al. (2004) imposed the criterion
 338 that the correlation between pairs of series be larger than 0.6. Before computing the
 339 correlation, we subtracted the trend and deseasonalized each record. Figure 2 shows that the

340 adjacent tide gauge records are highly correlated. The correlation coefficients fulfilled the
341 Kuo et al. (2004) criterion with 87% of the pairs of adjacent series displaying correlations
342 superior to 0.8, indicating a good agreement between the observed relative sea level variations
343 at neighboring tide gauges. A strong correlation is believed to indicate coherent fluctuations in
344 absolute sea level at two neighbouring tide gauges.

345 **Figure 2**

346 Fig.2: Correlation coefficients between the pairs of monthly tide gauge time series in the Gulf of Mexico (annual
347 and semi-annual cycles removed prior to calculation).

348 Table 2 (column 3) provides the vertical land movement estimates with formal errors obtained
349 at the selected 15 tide gauges in the Gulf of Mexico.

350 **3.3 Choice of the altimetry-tide gauge collocated points**

351 The satellite altimetry points were searched within a radius of one degree around the tide
352 gauge stations. Table 2 (Column 2, in parenthesis) shows the correlation coefficients between
353 the highest correlated satellite grid point and the tide gauge sea-level time series at the
354 selected 15 tide gauge stations. The annual and semi-annual cycles were removed prior to
355 calculation (section 2). It is also worth noting that the distance separating tide gauge station
356 and the corresponding altimetry grid point is not a key criterion in searching the coherent sea
357 level signals. In this study, high correlation coefficients were found for points located at
358 distances larger than 80 km (e.g., Galveston).

359 Despite the improvement in precision expected from the lengthening of the time series (there
360 are now 19 years of high-quality satellite altimetry data), the direct approach (e.g., Nerem and
361 Mitchum 2002; Fenoglio et al. 2004; Garcia et al. 2007; Ray et al. 2010; Braitenberg et al.
362 2011), results in the uncertainties of the estimated vertical land movements rates exceeding 1
363 mm/yr. Adding a couple of years of satellite altimetry data yielded only slight improvements

364 to the vertical rate estimates, far from the sub-millimeter accuracy required for many
365 geophysical applications (Pugh, 1987; Trisirisatayawong et al. 2011) . So, briefly, thus, the
366 implementation of the direct approach is restricted by the length of satellite time series and
367 not by that of tide gauge record. For this study, we chosed the altimetry grid point displaying
368 the highest correlation with the tide gauge under consideration. Errors in equations (E1) and
369 (E2) were assumed negligible as far as the long-term trend is concerned, the relative short
370 time span being the primary limitation affecting the land movement uncertainties.

371

372 **4. Results and discussion**

373

Table 2

374 Table 2: Geocentric vertical land movements at tide gauge sites using the combination of satellite altimetry data
375 and long term tide gauge records in the Gulf of Mexico. For comparison, GPS velocities nearby the tide gauge
376 are given, where available, from the ULR solution (Santamaría-Gómez et al. 2012), as well as GIA predictions
377 from Peltier (2004). Values are in mm/yr. Positive rate values mean land uplift while negative values mean land
378 subsidence.

379

380 4.1 Robustness checks

381

382 Table 2 presents the computed vertical land movement trends along with the GPS
383 measurements and the predictions of the post-glacial rebound model ICE5G-VM2 (Peltier,
384 2004). The direct approach yielded a formal uncertainty comprised between 0.7 and 0.8
385 mm/yr that is slightly better than uncertainties of previously published estimations mentioned
386 earlier. The uncertainty was reduced to 0.4 mm/yr in the advanced approach. At some tide
387 gauges the estimates of vertical land motion obtained by the direct and advanced approach
388 deviate substantially with difference of up to 5 mm/yr at Freeport.

389 Figure 3 exhibits vertical land movement rates in the northern Gulf of Mexico ranged between
390 -7.1 mm/yr (subsidence) and $+0.6$ mm/yr (uplift) as computed by the advanced approach.
391 Several robustness tests of the land movement estimates were carried out. For instance,
392 including the sea level data of 2011 or discarding that of 2009 yielded differences inferior to
393 0.2 mm/yr by using the advanced approach and as much as 1.5 mm/yr with the direct method.
394 An important issue is which altimetry data point should be taken to subtract the ocean sea
395 level signal from the tide gauge record? Selecting the closest grid point to the tide gauge
396 location instead of the most correlated one, or averaging the sea level anomalies from satellite
397 altimetry within a radius of 1 degree from the tide gauge, yielded differences of about 0.2
398 mm/yr using the advanced method, whereas the direct approach resulted in differences of 0.05
399 to 1 mm/yr. Here too, the differences were consistent with the associated error bars.

400

401 4.2 Comparison with the ICE-5G-VM2

402

403 The ongoing GIA induces a broad scale subsidence of the Gulf coasts
404 at a rate of about 0.5 - 1 mm/yr (Table 2) as estimated by ICE 5G VM2 model
405 (Peltier, 2004). The results obtained from both the direct and advanced
406 methods reveal significant deviations from the ICE 5G VM2 predictions
407 indicating strong local drivers of land movement at the Gulf coast
408 (e.g., Emery and Aubrey, 1991). The best correspondence between the results
409 of the advanced method and ICE 5G VM2 is obtained in Florida where the GIA
410 estimates fall in the uncertainty interval of the observed vertical land
411 movements at St. Petersburg, Fort Myers and Kew West. One can suggest that
412 ICE 5G VM2 predicts a somewhat faster subsidence in the South Florida
413 (-0.8 - -0.9 mm/yr) seen by the advanced method but the error bars

414 of our estimates seem to be too large to draw this conclusion. Notice,
415 however, that the tendency in the northward increasing of subsidence
416 from Naples to St Petersburg predicted by ICE 5G VM2 is quite close to
417 that measured by the advanced method.

418

419 4.3 Comparison with the GPS observations

420

421 A way of checking the reliability of the land movement estimates is to compare them to
422 independent measurements such as vertical velocities derived from relevant GPS solutions
423 (column 4 in Table 2 and Fig. 3) from the latest ULR solution described in section 2.
424 Comparison with GPS should be carried out with care because, the time span of GPS is much
425 shorter than that of the longest tide gauges in the GOM. By consequence, the GPS give
426 estimate of land movement vertical trends over last 10-15 years at maximum. The advanced
427 method gave a closer match to the GPS data at Galveston and at Grand Isle. It is interesting to
428 note that Kolker et al (2011) have obtained similar subsidence rates, 7.6 mm/yr at the Grand
429 Isle and 4.7 mm/yr at Galveston, by an independent technique: they assumed the Pensacola
430 tide gauge to be stable and subtracted it from Grand Isle and Galveston gauges. Our study
431 justifies, in some sense, the assumption made by Kolker et al. (2011) as the Pensacola
432 subsides very slowly (-0.2 mm/yr) according to the advanced method.

433 A somewhat larger vertical rate measured by the GPS at Galveston and at Grand Isle than that
434 derived from the advanced method might be interpreted as an acceleration of subsidence over
435 the past decade but this assumption would contradict other observations. Indeed, the
436 Galveston subsidence was recognized to be driven by water withdrawals (Kolker et al. 2011;
437 Meckel, 2008) which have decreased since 1970s (Meckel, 2008). As to Grand Isle, its
438 subsidence is mostly controlled by the Mississippi sediment loading (Ivins et al. 2007; Blum

439 et al. 2008) and should be more or less stable over the duration of tide gauge record used in
440 this study (Kolker et al. 2011). Also, the slowing of the wetlands loss in Barataria Bay
441 (Couvillion et al. 2011) indicates a slower vertical land motion at Grand Isle (Kolker et al.
442 2011). At Pensacola, the direct approach is more consistent with the GPS solution velocity
443 than the advanced approach. All GPS vertical rates are above the straight line in Fig.3
444 implying a small offset between the vertical movement given by the advanced method and the
445 GPS observations. It is difficult to find whether it is just a coincidence and all GPS stations
446 are situated in the regions lifting up faster than their long term trend. Theoretically, it can be
447 due as well to temporal fluctuations of the ITRF2008 reference frame (Beckley et al. 2007
448 The last row of Table 2 displays the scattering of the differences with the GPS velocities of
449 the ULR solution. The advanced approach showed a scattered difference with GPS velocities
450 of 0.4 mm/yr (Table 2), whereas it was of 1.5 mm/yr for the direct approach, confirming the
451 robustness of the advanced approach. Figure 4 supplements the comparison presented in the
452 previous section, highlighting the outlier behavior of the GPS velocity nearby Dauphin Island.
453 The error bars of the direct approach are too large to detect this outlier.

454

455 4.4 The drivers of vertical land motion along the Gulf coasts

456

457 The Texas coast from Port Isabel to Galveston II presents the greatest range in the relative sea
458 level rate (table 1) and in the rate of vertical land movement (table2). The rate of subsidence
459 increases from Port Isabel to Galveston by changing from -1.9 to -4.2 mm/yr with the
460 pronounced subsidence in Freeport (-7 mm/yr). This can be explained by different factors
461 impacting on the coast. The area to the southwest of Houston area has thinner sediment
462 accumulations and only modest petroleum production, and this contributes to minor
463 subsidence rates than those in East Texas (Buckley et al. 2003). The East Texas area,

464 including Freeport and Galveston is directly influenced by the fluid withdrawals due to a
465 combination of oil and gas extraction (Davis, 2011). An additional compaction factor is
466 caused by the area which includes many fairly large rivers that have carried abundant
467 sediment to the coast not as much as the Mississippi Delta area; but compaction from
468 sediment discharge plays also an important role in subsidence.

469 The Mississippi Delta area presents the highest vertical rates at Grand Isle. Grand Isle is
470 located over a barrier island directly exposed to the Mississippi river discharge. The size and
471 location of the barriers have changed considerably during historical time and barriers are
472 always reworking to form other vulnerable barriers (Davis, 2011). The processes driving
473 subsidence in Coastal Louisiana could be categorized in 6 elements: tectonic, Holocene
474 sediment compaction, sediment loading, glacial isotactic adjustment, anthropogenic fluid
475 withdrawal and surface water drainage and management (Yuill et al. 2009). The complexity of
476 estimating the subsidence rates in this area is due to the multiple physical processes
477 contributing to subsidence, all of which occur at their own distinct spatial and temporal scales
478 (Meckel, 2008). Ivins et al. (2007) found in the area of Grand Isle a rate of subsidence of 6.3
479 ± 1.9 mm/yr caused by the Mississippi sediment loading that is compatible with our results
480 (table 2).

481 The Northeastern Gulf coast contains two large streams, the Mobile River and the
482 Apalachicola River, this river have deposited a considerable amount of sediment along the
483 coast contributing to compaction along the coast and consequently to a rate of subsidence
484 from 2.4 to 4 mm/yr (Davis, 2011). This rate does not match well with the rates of Dauphin
485 Island and Apalachicola stations which are twice as large as the subsidence rates of each tide
486 gauge station.

487 The small vertical land rates in Florida could be partially explained by the geologic context of
488 the peninsula. Indeed, the Florida peninsula is a carbonate platform far away from tectonic

489 activity and does not receive sediment runoff from the nearby continent (Dokka, 2006). The
490 rates of land movement are small compared to the Texas and the Mississippi Delta areas (table
491 2). The changes in vertical land movement rates could be explained partly by the model of
492 GIA.

493 On the Mexico coast, near Veracruz, the rate of relative sea level rise is probably influenced
494 by the proximity of volcanic activity (Cantagrel and Robin, 1978). Little deviation from rate
495 is observed in the sea level rise at Veracruz, the vertical rate being about 0.2 ± 0.5 mm/yr at
496 Veracruz.

497

498

499 4.5 A crustal uplift between Cedar Key and Pensacola?

500

501 There is a noticeable discrepancy between the ICE5G-VM2 predictions and the advanced
502 model vertical rates from Cedar Key II to Pensacola. At all TGs, from Key West to St.
503 Petersburg, the ICE5G-VM2 predictions are within the error bars of the advanced model but
504 the GIA-induced subsidence is disagreement with the advanced model. According to Ivins et
505 al (2007) Dauphin Island and Pensacola are subject to additional subsidence of about 1.5 – 2
506 mm/yr due to loading by Mississippi sediment. So, the subsidence at Dauphin Island and
507 Pensacola is expected to be stronger than the GIA predictions. Contrarily, the advanced
508 method estimates a slower subsidence or even a crustal uplift at Cedar Key – Apalachicola.
509 This suggests a local driver that could contribute to a crustal uplift between Cedar Key and
510 Pensacola. Searching for causes of this uplift is beyond the scope of our study although some
511 active fault in this region could probably induce it (Dokka, 2006). Shinkle and Dokka (2004)
512 and Dokka (2006) have detected uplift in Pensacola region from the leveling data due,
513 probably, to tectonic processes as salt migration or regional warping induced by sedimentation

514 loading. Also, it is worth of noticing, that the Apalachicola TG is situated in the vast flood
515 plain and the difference between sea level measured at Cedar Key and Apalachicola can be
516 caused by sediment accretion/erosion processes. Certainly, even if the difference in vertical
517 land movement between these two tide gauges really exists, it is very weak and asks for
518 much more detailed exploration through other geophysical data.

519

520

521

522

523

524 **Figure 3**

525 Fig. 3: Geocentric vertical land movements at tide gauge sites using the advanced combination of satellite
526 altimetry data over the period 1992-2011 and long term tide gauge records over their covered period in the Gulf
527 of Mexico. GPS velocities nearby the tide gauge are given, where available. Values are in mm/yr.

528

529

530 **Figure 4**

531 Fig.4: Comparison of vertical land movements derived from the direct and advanced combinations of satellite
532 altimetry and tide gauge data with GPS vertical velocities from the ULR solution at the five co-located stations
533 (see Table 1 and text section 2.3). Error bars of 1-sigma are indicated.

534

535 **5. Conclusions**

536 A method combining the tide gauge records and the satellite altimetry data (Kuo et al. 2004)
537 was used in order to estimate the vertical land movement rates at tide gauge stations along the

538 Gulf of Mexico coast. The method was shown to yield highly consistent estimates and to be
539 more precise than a straightforward subtraction of the altimetry data from tide gauge records.
540 An averaged bias of about 0.8 mm/yr was revealed from the comparison of the estimated
541 vertical land movement rates with the GPS measurements. As the subsidence rates in
542 Louisiana and Texas seemed to be on decline over the last 40 years, this bias is probably an
543 indication of the error due to temporal variability of the ITRF reference frame. This method
544 should be considered as a useful tool for assessing vertical land movement rates.

545 The highest vertical land motion rates were estimated at Freeport (7.0 mm/yr) and Grand Isle
546 (7.1 mm/yr). We suggested that slow subsidence of Pensacola (-0.2 mm/yr), as well as a small
547 but noticeable uplift of Apalachicola and Cedar Key is a manifestation of some local tectonic
548 motion. The method of Kuo et al. assumes that the absolute sea level trend does not change
549 between neighbouring tide gauges. If this hypothesis is not justified, then the non-negligible
550 difference between the absolute sea level trends at two stations will be attributed to the
551 difference in vertical tide gauge movement and, by consequence, the vertical land motion
552 trends will be over/under estimated. In the present study, we feel confident in the basic
553 assumption of Kuo et al method, as the largest distance between tide gauges in the GOM is
554 about 780 km and the low-frequency sea level perturbations propagate over the whole shelf
555 in the GOM in about one month as demonstrated by Li and Clark (2005). The length of the
556 tidal records (> 46 years) assures, on the other hand, an accurate estimation of trends by the
557 least square procedure (Table 2).

558 We corrected the tide gauge records from the vertical land rates and estimated the absolute sea
559 level rise to be of about 2.0 ± 0.4 mm/yr. This value is comparable to the global absolute sea
560 level rise estimates over the last 50 years (Church and White, 2011) : 1.9 ± 0.4 mm/yr over the
561 period 1961-2009. Hopefully, this additional case study will increase the interest for this
562 technique, and contribute to obtain worthwhile results in other geographical contexts. In this

563 respect, the application of the advanced approach to other regions and oceanic contexts will
564 certainly provide invaluable insights to the nature of tectonic and anthropogenic processes
565 driving the coastal land motion.

566

567 **Acknowledgements**

568 The work presented in this article was supported by the French Research National Agency
569 (ANR) through the CEP-2009 program (Project ‘Coastal Environmental Changes: Impact of
570 sea LEvel rise’ (CECILE) under grant number ANR-09-CEP-001-01). It was also partly
571 funded by *Région Poitou-Charentes*, which provided a PhD fellowship for C. Letetrel and by
572 Universitat de les Illes Balears, which provided a visiting professor grant for G. Wöppelmann.
573 M. Marcos acknowledges a “Ramon y Cajal” contract funded by the Spanish Ministry of
574 Science. The four anonymous reviewers are also acknowledged for their constructive
575 comments. The altimetry data used herein were distributed by AVISO, with support from the
576 French space agency CNES. We would like to thank CLS contacts for their prompt and
577 efficient on-line user’s support. The tide gauge data were provided by the Permanent Service
578 for Mean Sea Level (PSMSL) and the GPS data were distributed by CORS and IGS, which
579 benefit from the support of many agencies. We also thank the SONEL data assembly center
580 for providing a comprehensive and easy access to the GPS data at tide gauges used in this
581 study.

582 **References**

- 583 Altamimi, Z., Collilieux X., Métivier, L., 2011. ITRF2008: an improved solution of the international terrestrial reference
584 frame. *Journal of Geodesy*, 85 (8), p. 457-473. doi: 10.1007/s00190-011-0444.
- 585 Ablain, M., Cazenave, A., Valladeau, G., Ginehut, S., 2009. A new assessment of the error budget of global mean sea level
586 rate estimated by satellite altimetry over 1993-2008. *Ocean Science*, 5, p. 193-201.

587 Beckley, B.D., Lemoine, F.G., Luthcke, S.B., Ray, R.D., Zelensky, N.P., 2007. A reassessment of global and regional mean sea
588 level trends from TOPEX and Jason-1 altimetry based on revised reference frame and orbits. *Geophys. Res. Lett.*, 34,
589 L14608. doi:10.1029/2007GL030002.

590 Blewitt, G., Altamimi, Z., Davis, J.L., Gross, R.S., Kuo, C., Lemoine, F., Moore, A.W., Neilan, R., Plag, H., Rothacher, M.,
591 Shum, C., Sideris, M., Schöne, T., Tregoning, P., Zerbini, S., 2010. Geodetic observations and global reference frame
592 contributions to understanding sea level rise and variability. In: Church J., Woodworth P.L., Aarup T., Wilson S. (eds)
593 *Understanding sea level Rise and variability*. Wiley-Blackwell, London, p 256-284.

594 Blum, M.D., Tompkin, J.H., Purcell, A., Lancaster, R.R., 2008. Ups and downs of the Mississippi Delta. *Geology*, v. 36, p.
595 675-678.

596 Boesch, D.E., Josslyn, M.N., Mehta, A.J., Morris, J.T., Nuttle, W.K., Simestad, C.A., Swift, D.J., 1994. Scientific Assessment
597 of Coastal Wetland Loss, Restoration and Management in Louisiana. *J. Coastal Res.*, Special Issue no. 20, 103 pp.

598 Bouin, M.N., Wöppelmann, G., 2010. Land motion estimates from GPS at tide gauges: a geophysical evaluation. *Geophysical*
599 *Journal International*, 180, p. 193-209.

600 Braitenberg, C., Mariani, P., Tunini, L., Grillo, B., Nagy, I., 2011. Vertical crustal motions from differential tide gauge
601 observations and satellite altimetry in southern Italy. *Journal of Geodynamics*, 51, p. 233-244.

602 Buble, G., Bennett, R.A., Hreinsdóttir, S., 2010. Tide gauge and GPS measurements of crustal motion and sea level rise along
603 the eastern margin of Adria. *J. Geophys. Res.*, 115, B02404, doi:10.1029/2008JB006155.

604 Buckley, S.M., Rosen, P.A., Hensley, S., Tapley, B.D., 2003. Land subsidence in Houston, Texas, measured by radar
605 interferometry and constrained by extensometers. *J. Geophys. Res.*, 108(B11), 2542, doi:10.1029/2002JB001848.

606 Cantagrel, J.M., Robin, C., 1978. K-Ar dating on eastern Mexican volcanic rocks — Relations between the andesitic and the alkaline
607 provinces *Journal of Volcanology and Geotherman Research*, 5(1-2), p. 99-114.

608 Carrère, L., Lyard, F., 2003. Modeling the barotropic response of the global ocean to atmospheric wind and pressure forcing -
609 comparisons with observations. *Geophys. Res. Lett.*, 30(6), 1275, doi: 10.1029/2002GL016473.

610 Cazenave, A., Dominh, K., Ponchaut, F., Soudarin, L., Crétaux, J.F., Le Provost, C., 1999. Sea level changes from Topex-
611 Poseidon altimetry and tide gauges, and vertical crustal motions from DORIS. *Geophys. Res. Lett.*, 26, p. 2077-2080.

612 Church, J. A., White, N.J., 2011. Sea-level rise from the late 19th to the early 21st Century. *Surveys.Geophysics*, 32, p. 585-
613 602, doi:10.1007/s10712-011-9119-1.

614 Collilieux, X., Wöppelmann, G., 2011. Global sea level rise and its relation to the terrestrial reference frame definition.
615 *Journal of Geodesy*, 85, p. 9-22.

616 Couvillion, B.R., Barras, J.A., Steyer, G.D., Sleavin, W., Fischer, M., Beck, H., Trahan, N., Griffin, B., Heckman, D., 2011.
617 Land area change in coastal Louisiana from 1932 to 2010. U.S. Geological Survey Scientific Investigations Map 3164, scale
618 1:265,000, 12 pp.. pamphlet.

619 Crosset, K.M., Culliton, T.J., Wiley, P.C., Goospeed, T.R., 2004. Population trends along the coastal United States. Coastal
620 trends report series, NOAA Technical Report, 54 pp.

621 Davis, J.L., Mitrovica, J.X., Scherneck, H.G., Fan, H., 1999. Investigations of Fennoscandian glacial isostatic adjustment
622 using modern sea level records. *Journal of Geophysical Research*, 1004 (B2), p. 2733-2747.

623 Davis, R.A. Jr., 2011. Sea-level change in the gulf of Mexico. Texas A&M University Press, College station. 172 pp.

624 Dokka, R.K., 2006. Modern-day tectonic subsidence in coastal Louisiana. *Geology*, 34, p. 281–284.

625 Douglas, B.C., 1991. Global sea level rise. *J. Geophys. Res.*, 96 (C4), p. 6981-6992.

626 Douglas, B.C., 2001. Sea level change in the era of the recording tide gauge. In *Sea Level Rise: History and Consequences*,
627 *Int. Geophys. Ser.*, vol.75, edited by Douglas, B., Kearney, M., and Leatherman, S., chap.3, Academic, San Diego, p. 37-64.

628 Douglas, B.C., 2005. Gulf of Mexico and Atlantic coast sea level change. In *Circulation in the Gulf of Mexico: observations*
629 *and models*, *Geophysical Monograph Series*, 161, edited by Sturges, W., and Lugo-Fernandez, A., p. 111-121.

630 Emery, K.O., Aubrey, D.G., 1991. Sea levels, land levels, and tide gauges. Springer Verlag, 237 pp.

631 Fenoglio-Marc, L., Dietz, C., Groten, E., 2004. Vertical land motion in the Mediterranean Sea from altimetry and tide gauge
632 stations. *Marine Geodesy*, 27, p. 683-701, doi: 10.1080/01490410490883441.

633 Garcia, D., Vigo, I., Chao, B.F., Martinez, M.C., 2007. Vertical crustal motion along the Mediterranean and Black Sea coast
634 derived from ocean altimetry and tide gauge data. *Pure and Appl. Geophys.*, 64, p. 851-863.

635 Gonzalez, J.L., Törnqvist, T.E., 2006. Coastal Louisiana in crisis : subsidence or sea level rise?. *EOS, Transactions, American*
636 *Geophysical Union*, 87, p. 493–498.

637 Holgate S.J., Matthews, A., Woodworth, P.L., Rickards, L.J., Tamisiea, M.E., Bradshaw, E., Foden, P.R., Gordon,
638 K.M., Jevrejeva, S., Pugh, J., 2013. New Data Systems and Products at the Permanent Service for Mean Sea Level. *J. Coastal*
639 *Res.*, 29 (3), p. 493-504. doi:10.2112/JCOASTRES-D-12-00175.

640 Holgate, S.J., Woodworth, P.L., 2004. Evidence for enhanced coastal sea level rise during the 1990s. *Geophys. Res. Lett.*, 31,
641 L07305, doi:10.1029/2004GL019626.

642 Ivins, E.R., Dokka, R.K., Blom, R.G., 2007. Post-glacial sediment load and subsidence in coastal Louisiana. *Geophys. Res.*
643 *Lett.*, 34, L16303, doi:10.1029/2007GL030003.

644 Kolker, A.S., Allison, M.A., Hameed, S., 2011. An evaluation of subsidence rates and sea level variability in the northern
645 Gulf of Mexico. *Geophys. Res. Lett.*, 38, L21404, doi:10.1029/2011GL049458.

646 Kuo, C.Y., 2005. Determination and characterization of the 20th century global sea level rise. Ph.D., The Ohio State
647 University, U.S., 250 pp.

648 Kuo, C.Y., Shum, C.K., Braun, A., Mitrovica, J.X., 2004. Vertical crustal motion determined by satellite altimetry and tide
649 gauge data in Fennoscandia. *Geophys. Res. Lett.*, 31, L01608, doi: 10.1029/2003GL019106.

650 Kuo, C.Y., Shum, C.K., Braun, A., Cheng, K.C., Yi, Y., 2008. Vertical motion determined using satellite altimetry and tide
651 Gauges. *Terr. Atmos. Ocean. Sci.*, 19, p. 21-35, doi:10.3319/TAO.2008.19.1-2.21(SA).

652 Letetrel, C., 2010. Mouvements verticaux à la surface de la Terre par altimétrie radar embarquée sur satellite, marégraphie et
653 GPS. : un exemple d'application : le Golfe du Mexique. Ph.D., Université of La Rochelle, France, 185 pp.

654 Li, J., Clarke, A.J., 2005. Interannual flow along the northern coast of the Gulf of Mexico. *Journal of Geophysical Research*,
655 110, C11002, doi: 10.1029/2004JC002606.

656 Lopez, J.A., 1991. Origin of Lake Pontchartrain and the 1987 Irish Bayou earthquake. *Gulf Coast Sect. SEPM, 12th Annual*
657 *Research Conference*, p. 103–110.

658 Meckel, T.A., 2008. An attempt to reconcile subsidence rates determined from various techniques in southern Louisiana.
659 *Quaternary Science Reviews*, v. 27, p. 1517-1522.

660 Menke, W., 1989. *Geophysical data analysis: discrete inverse theory*. Academic Press, 289 pp.

661 Mitchum, G.T., 1994. Comparison of TOPEX sea surface heights and tide gauge sea levels. *J. Geophys. Res.*, 99 (C12), p.
662 24541–24553, doi:10.1029/94JC01640.

663 Mitchum, G.T., 1998. Monitoring the stability of satellite altimeters with tide gauges. *Journal of Atmospheric and Oceanic*
664 *Technology*, 15, p. 721-730.

665 Mitrovica, J.X., Milne, G.A., 2002. On the origin of late Holocene sea-level highstands within equatorial ocean basins.
666 *Quaternary Science Reviews*, v. 21, p. 2179-2190.

667 Nerem, R., Mitchum, G., 2002. Estimates of vertical crustal motion derived from differences of TOPEX/POSEIDON and tide
668 gauge sea level measurements. *Geophys. Res. Lett.*, 29, 1934, doi: 10.1029/2002GL015037.

669 Nicholson, C., Wesson, R.L., 1990. Earthquake hazard associated with deep well injection; a report to the U.S.
670 Environmental Protection Agency. USGS Bulletin, 1951.

671 Oey, L.Y., Ezer, T., Lee, H.C., 2005. Loop current, rings and related circulation in the Gulf of Mexico: A review of numerical
672 models and future challenges in *Circulation*. In *Circulation in the Gulf of Mexico: observations and models*, Geophysical
673 *Monograph Series*, 161, edited by Sturges W., and Lugo-Fernandez, A., p. 31-56.

674 Peltier, W.R., 2004. Global Glacial Isostasy and the Surface of the Ice-Age Earth: The ICE-5G (VM2) model and GRACE.
675 *Annu. Rev. Earth. Planet. Sci.*, 32, p. 111-149, doi:10.1146/annurev.earth.32.08503.144359.

676 Pugh, D.T., 1987. *Tides, surges and mean sea-level: a handbook for engineers and scientists*. Wiley, Chichester, 472 pp.

677 Ray, R.D., Beckley, B.D., Lemoine, F.G., 2010. Vertical crustal motion derived from satellite altimetry and tide gauges, and
678 comparisons with DORIS. *Adv. Space Res.*, 45(12), p. 1510-1522.

679 Santamaría-Gómez, A., Bouin, M-N., Collilieux, X., Wöppelmann, G., 2011. Correlated errors in GPS position time series:
680 implications for velocity estimates. *Journal of Geophysical Research*, 116, B01405, doi:10.1029/2010JB007701.

681 Santamaría-Gómez A., Gravelle, M., Collilieux, X., Guichard, M., Martin Miguez, B., Tiphaneau, P., Wöppelmann, G., 2012.
682 Mitigating the effects of vertical land motion in tide gauge records using a state-of-the-art GPS velocity field. *Global and*
683 *Planetary Change*, Vol. 98-99, p. 6-17

684 Shinkle, K.D., Dokka, R.K., 2004. Rates of vertical displacement at benchmarks in the lower Mississippi Valley and the
685 northern Gulf Coast. *NOAA Tech. Rep.*, 50, 135 pp.

686 Stammer, D., 2008. Response of the global ocean to Greenland and Antarctic ice melting. *Journal of Geophysical Research*,
687 113, C06022, doi:10.1029/2006JC004079.

688 Street, J.O., Carroll, R.J., Ruppert, D., 1988. A note on computing robust regression estimates via iteratively reweighted least
689 squares. *The American Statistician*, 42, p. 152-154.

690 Sturges, W, Evans, J.C., 1983. On the variability of the Loop Current in the Gulf of Mexico. *Journal of Marine Research*, 41,
691 p. 639-653.

692 Törnqvist, T.E.; Bick, S.J, Van der Borg, K., De Jong, A.F.M., 2006. How stable is the Mississippi Delta?. *Geology* , 34, p.
693 697–700

694 Trisirisatayawong, I., Naeije, M., Simons, W., Fenoglio-Marc, L., 2011. Sea Level Change in the Gulf of Thailand from GPS-
695 corrected Tide Gauge Data and Multi-Satellite Altimetry. *Global and Planetary Change*, 76, p. 137-151,
696 doi:10.1016/j.gloplacha.2010.12.010.

697 Volkov, D.L., Larnicol, G, Dorandeu, J., 2007. Improving the quality of satellite altimetry data over continental shelves.
698 *Journal of Geophysical Research*, 112, C06020, doi: 10.1029/2006JC003765.

699 Woodworth, P.L., Player, R., 2003. The Permanent Service for Mean Sea Level: an update to the 21st century. *Journal of*
700 *Coastal Research*, 19, p. 287-295.

701 Wöppelmann, G, Martin Miguez, B., Bouin, M-N., Altamimi Z., 2007. Geocentric sea-level trend estimates from GPS
702 analyses at relevant tide gauges world-wide. *Global and Planetary Change*, 57, p. 396-406.

703 Wöppelmann, G, Letretel, C., Santamaría, A., Bouin, M.-N., Collilieux, X., Altamimi, Z., Williams, S., Martín Míguez, B.,
704 2009. Rates of sea-level change over the past century in a geocentric reference frame. *Geophys. Res. Lett.*, 36, L12607, doi:
705 10.1029/2009GL038720.

706 Wöppelmann, G, Marcos, M., 2012. Coastal sea level rise in southern Europe and the nonclimate contribution of vertical land
707 motion. *J. Geophys. Res.*, 117, C01007, doi:10.1029/2011JC007469.

708 Yuill, B., Lavoie, D., Reed, D.J., 2009. Understanding Subsidence Processes in Coastal Louisiana. *Journal of Coastal*
709 *Research*. 54, p. 23-26.

710

711 **Figure captions**

712 Fig.1: Location of tide gauge records in the northern Gulf of Mexico (circles) with more than
713 40 years of data at PSMSL and grid points from AVISO altimetry data used in this study. The
714 background colours represent sea level rates over the common period October 1992 to
715 December 2011. The underlined tide gauge names denote the co-location with a nearby
716 continuous GPS station.

717 Fig.2: Correlation coefficients between pairs of monthly tide gauge time series in the Gulf of
718 Mexico (annual and semi-annual cycles removed prior to calculation).

719 Fig.3: Geocentric vertical land movements at tide gauge sites using the advanced combination
720 of satellite altimetry data over the period 1992-2011 and long term tide gauge records over
721 their covered period in the Gulf of Mexico. GPS velocities nearby the tide gauge are given,
722 where available. Values are in mm/yr.

723 Fig.4: Comparison of vertical land movements derived from the direct and advanced
724 combinations of satellite altimetry and tide gauge data with GPS vertical velocities from the
725 ULR solution at the five co-located stations (see Table 1 and text section 2.3). Error bars of 1-
726 sigma are indicated.

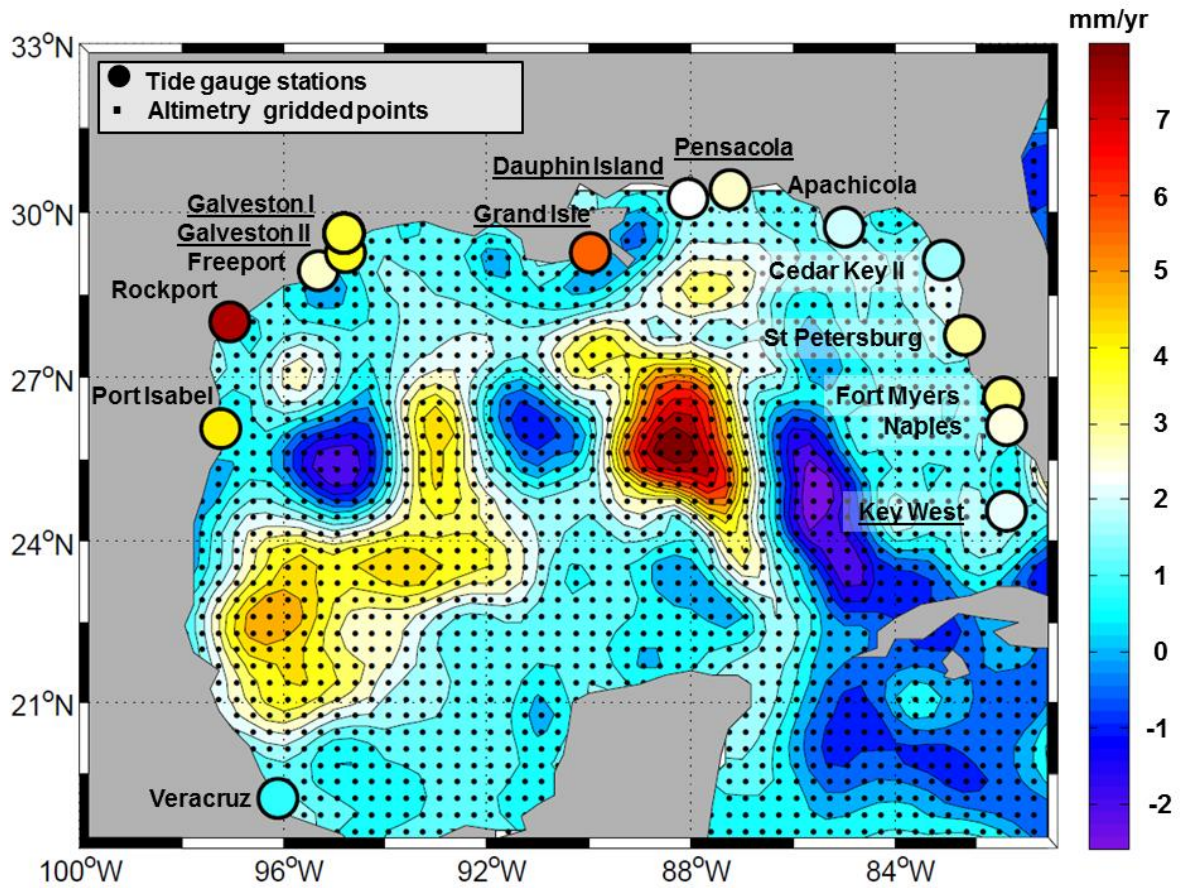
727

728 **Table captions**

729 Table 1: Tide gauge data used in this study from the PSMSL. Trend values and standard errors
730 of the trends (in mm/yr) are derived from a robust linear regression (Street et al. 1988) over
731 the entire data span available at each tide gauge. Approximate distances to the nearby
732 continuous GPS station are in km.

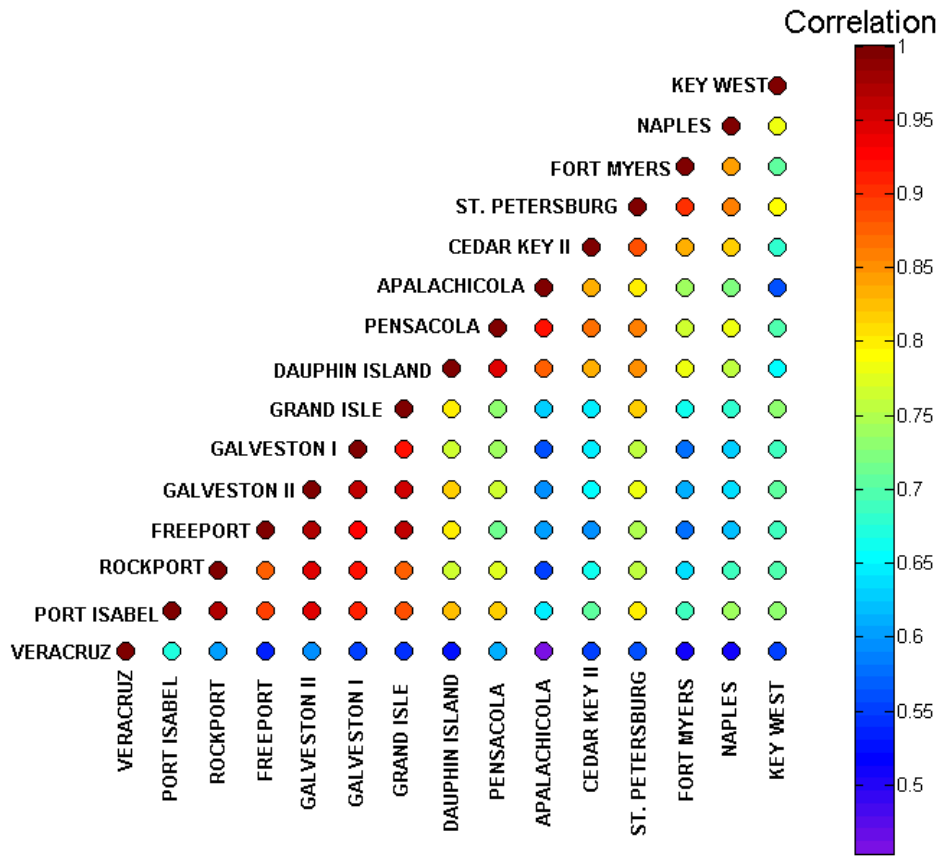
733 Table 2: Geocentric vertical land movements at tide gauge sites using the combination of
734 satellite altimetry data and long term tide gauge records in the Gulf of Mexico. For
735 comparison, GPS velocities nearby the tide gauge are given, where available, from the ULR

736 solution (Santamaría-Gómez et al. 2012), as well as GIA predictions from Peltier (2004).
737 Values are in mm/yr. Positive rate values mean land uplift while negative values mean land
738 subsidence.
739



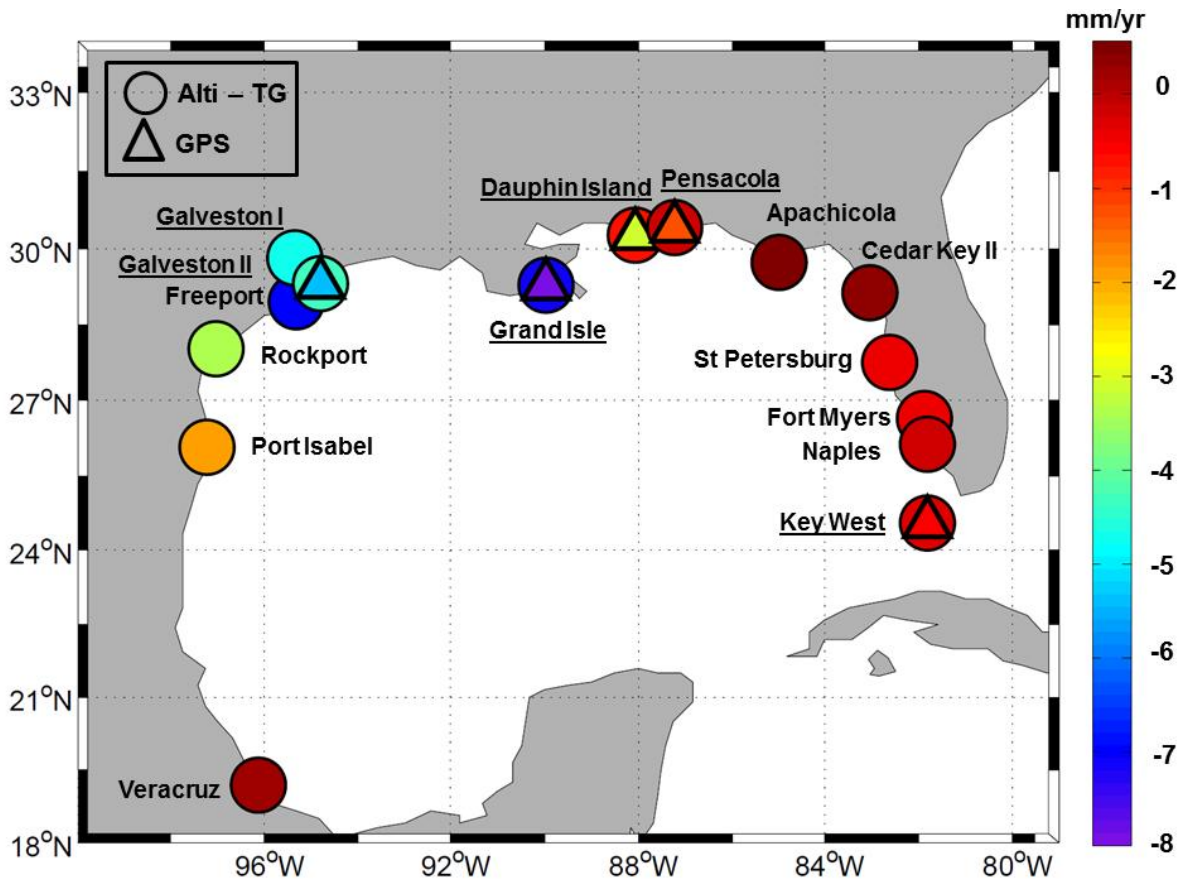
740

741



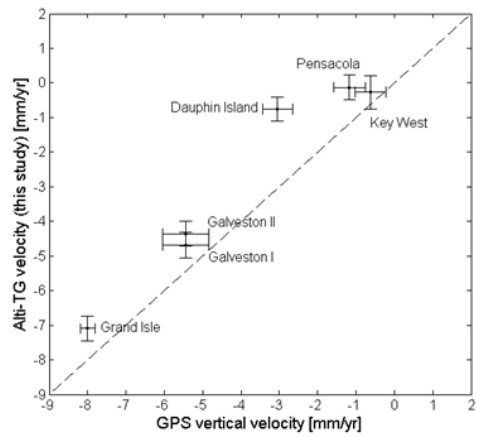
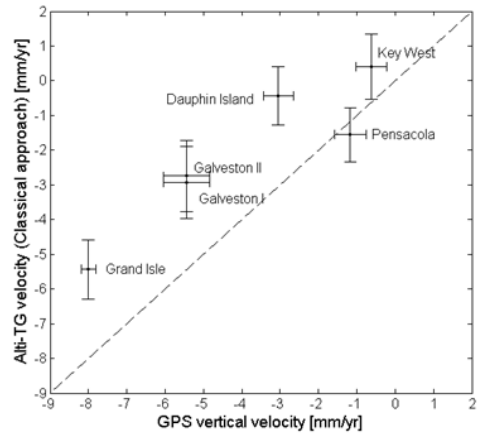
742

743



744

745



746